Electronic Supplementary Information for:

Macromolecular Helicity Control of Poly(phenyl isocyanate)s with Single Stimuli-Responsive Chiral Switch

Mayu Fukuda,‡[a] Rafael Rodríguez,‡[b] Zulema Fernandez,[c] Tatsuya Nishimura,[a] Daisuke Hirose,[ab] Go Watanabe,[d] Emilio Quiñoá,[c] Félix Freire*[c] and Katsuhiro Maeda*[ab]

[a]Graduate School of Natural Science and Technology Kanazawa University, Kakuma-machi, Kanazawa 920-1192, Japan

[b]WPI Nano Life Science Institute (WPI-NanoLSI), Kanazawa University, Kakuma-machi, Kanazawa 920-1192, Japan

[c]Centro Singular de investigación en Química Biolóxica e Materiais Moleculares (CiQUS) and Departamento de Química Orgánica, Universidade de Santiago de Compostela, 15782, Santiago de Compostela, Spain.

[d]School of Science, Kitasato University, 1-15-1 Kitasato, Minami-Ku, Sagamihara, Kanagawa 252-0373, Japan

Table of Contents

1. Instruments

NMR spectra were recorded on JEOL ECA500 (500 MHz for ^{1}H, 125 MHz for ^{13}C) or LA400 (400 MHz for ^{1}H) spectrometers (Tokyo, Japan) in $CDCl_3$ using TMS as an internal standard. The size exclusion chromatography (SEC) measurements were performed with a JASCO PU-4180 liquid chromatograph equipped with a RI detector (JASCO RI-4030) and a column oven (JASCO CO-4060) (Hachioji, Japan). The number- (M_n) and weight-average (M_w) molecular weights of polymers were determined at 40 °C using a Shodex KF-805L SEC column (Tokyo, Japan), and THF was used as the eluent at a flow rate of 1.0 mL/min. The molecular weight calibration curve was obtained using polystyrene standards (Tosoh, Tokyo, Japan). Absorption and circular dichroism (CD) spectra were measured in a quartz cell with a path length of 0.1 or 0.5 cm on a JASCO V-650 spectrophotometer and a JASCO J-725 spectropolarimeter, respectively. The temperature was controlled with a JASCO ETC 505T (for absorption spectral measurements) and a JASCO 348WI apparatus (–10—20 °C) or a liquid nitrogen-controlled quartz cell (5.0 mm) in a cryostat (–100—20 °C) (for CD spectral measurements). IR spectra were recorded with a JASCO Fourier Transform IR-460 spectrophotometer on ATR mode. VCD experiments were performed on a Jasco FVS-6000, using deuterated solvents in a pre-mounted cell with BaF_2 lens of 150 μm path length. Spectra was recorded over an average of 6000 scans. The concentration of the sample was 30 mg/mL. Elemental analyses were performed by the Research Institute for Instrumental Analysis of Advanced Science Research Center, Kanazawa University, Kanazawa, Japan.

2. Materials

(*R*)- and (*S*)-*α*-methoxyphenylacetic acid ((*R*)- and (*S*)-MPA), aniline, acetyl chloride, and 3-methoxyphenylisocyanate (3-MeOPI) were purchased from Tokyo Chemical Industry (TCI, Tokyo, Japan). *N*,*N*-dimethyl-4-aminopyridine (DMAP) was purchased from Sigma-Aldrich (St. Louis, MO). 1-Ethyl-3-(3-dimethylaminopropyl)carbodiimide (EDC) was purchased from Oakwood Chemicals. Anhydrous THF and *n*BuLi (1.57 M in hexane) were purchased from Kanto Kagaku (Tokyo, Japan). Lithium triflimide ($LiNTf_2$), lithium triflate (LiOTf), lithium perchlorate ($LiClO_4$), and lithium tetrafluoroborate ($LiBF_4$) were obtained from TCI. Sodium tetrakis[3,5-bis(trifluoromethyl)phenyl]borate (NaBArF) was purchased from Carbosynth (Oxford, UK). Other BArF salts were synthesized using NaBArF and the corresponding chloride salts as the starting material by the conventional ion-exchange method.[S1] Otherwise stated the reagents were used without further purification from commercial source. 3-MeOPI was distilled over CaH_2 under reducer pressure prior to use as previously reported.[S2] The synthesis of poly-***3S*** with an (*S*)-2-(methoxymethyl)pyrrolidine ((*S*)-MMP) residue at the initial chain end have been previously reported (see run 3 in Table S1).[S2]

3. Synthetic Procedure

3.1. Synthesis of (*R*)-*N*-phenyl 2-Methoxyphenylacetamide (2*R*)

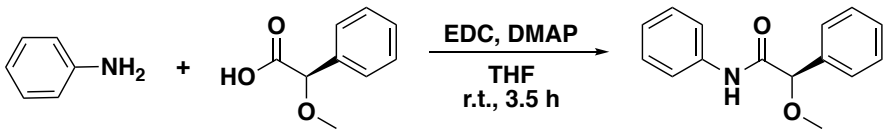

(*R*)-MPA (1.18 g, 7.10 mmol, 1.2 equiv.), EDC (1.70 g, 8.88 mmol, 1.5 equiv.) an DMAP (72.0 mg, 0.59 mmol, 0.1 equiv.) were dissolved in 40 mL of THF and the mixture was stirred for 15 min to activate the acid. Next, aniline (540 μL, 5.92 mmol, 1.0 equiv.) was added and the mixture was stirred for additional 3.5 h. The organic layer was washed with 1 M HCl (20 mL) and sat. $NaHCO_3$ (20 mL) and dried with Na_2SO_4. The organic solvent was evaporated under vacuum and the resulting crude was purified by chromatographic column with hexane/ethyl acetate (EtOAc) (3/2, v/v) as the eluent. The title compound was obtained in 99% yield. The enantiomeric excess (ee) value of the obtained **2*R*** was determined to be 96% ee by chiral HPLC analysis on CHIRALPAK AS-H (DAICEL, Tokyo, Japan) column (25 × 0.46 (i.d.) cm) with *n*-hexane–2-propanol (80/20, v/v) as the eluent at a flow rate of 0.8 mL/min at ca. 25 °C (254 nm, t_S = 8.4 min, t_R = 12.3 min). Mp 77.8-78.1 °C. IR (KBr): 1685 (amide I), 1528 (amide II) cm^{-1}. ^1H NMR (500 MHz, $CDCl_3$) δ 8.56-8.44 (m, 2H), 8.13-8.03 (m, 2H), 7.93-7.80 (m, 2H), 7.70-7.60 (m, 3H), 7.06-6.94 (m, 1H), 4.73 (s, 1H), 3.45 (s, 3H). ^{13}C NMR (125 MHz, $CDCl_3$) δ 168.6, 137.5, 136.7, 129.1, 128.8, 128.7, 127.2, 124.5, 119.7, 84.0, 57.5. HRMS (FAB) m/z calcd for $C_{15}H_{16}NO_2[M + H^+]$: 242.1176, found: 242.1182. $[\alpha]_D^{25}$ –56° (*c* 1.0, $CHCl_3$).

3.2. Synthesis of (*S*)-*N*-phenyl 2-Methoxyphenylacetamide (2*S*)

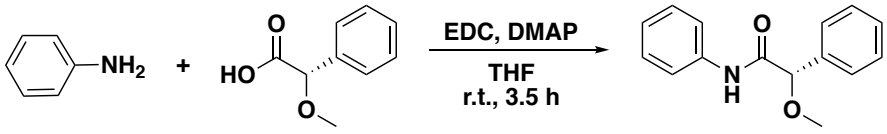

This compound was synthesized from (*S*)-MPA in the same way for the synthesis of **2*R***. The crude product was purified by chromatographic column with hexane/EtOAc (3/2) as eluent to give **2*S*** as a white solid in 90% yield. The ee of the obtained **2*S*** was determined to be 96% ee in the same way as for **2*R***. Mp 78.3-78.6 °C. IR (KBr): 1685 (amide I), 1528 (amide II) cm^{-1}. ^1H NMR (500 MHz, $CDCl_3$) δ 8.56-8.44 (m, 2H), 8.13-8.03 (m, 2H), 7.93-7.80 (m, 2H), 7.70-7.60 (m, 3H), 7.06-6.94 (m, 1H), 4.73 (s, 1H), 3.45 (s, 3H). ^{13}C NMR (125 MHz, $CDCl_3$) δ 168.6, 137.4, 136.7, 129.1, 128.8, 128.7, 127.2, 124.5, 119.7, 84.0, 57.5. HRMS (FAB) m/z calcd for $C_{15}H_{16}NO_2[M + H^+]$: 242.1176, found: 242.1179. $[\alpha]_D^{25}$ +58° (*c* 1.0, $CHCl_3$).

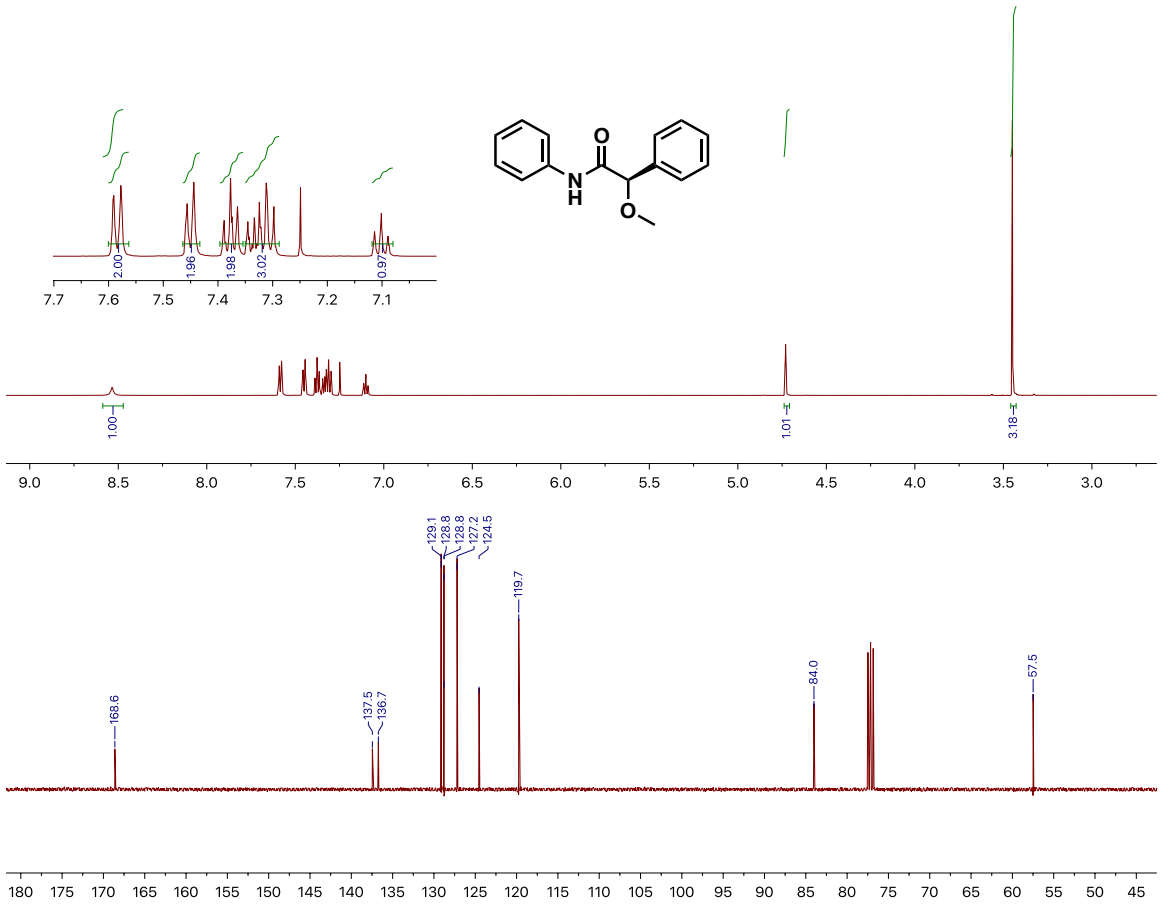

Figure S1. ^{1}H and ^{13}C NMR spectra of initiator **2*R*** in $CDCl_3$ (500 MHz and 125 MHz respectively).

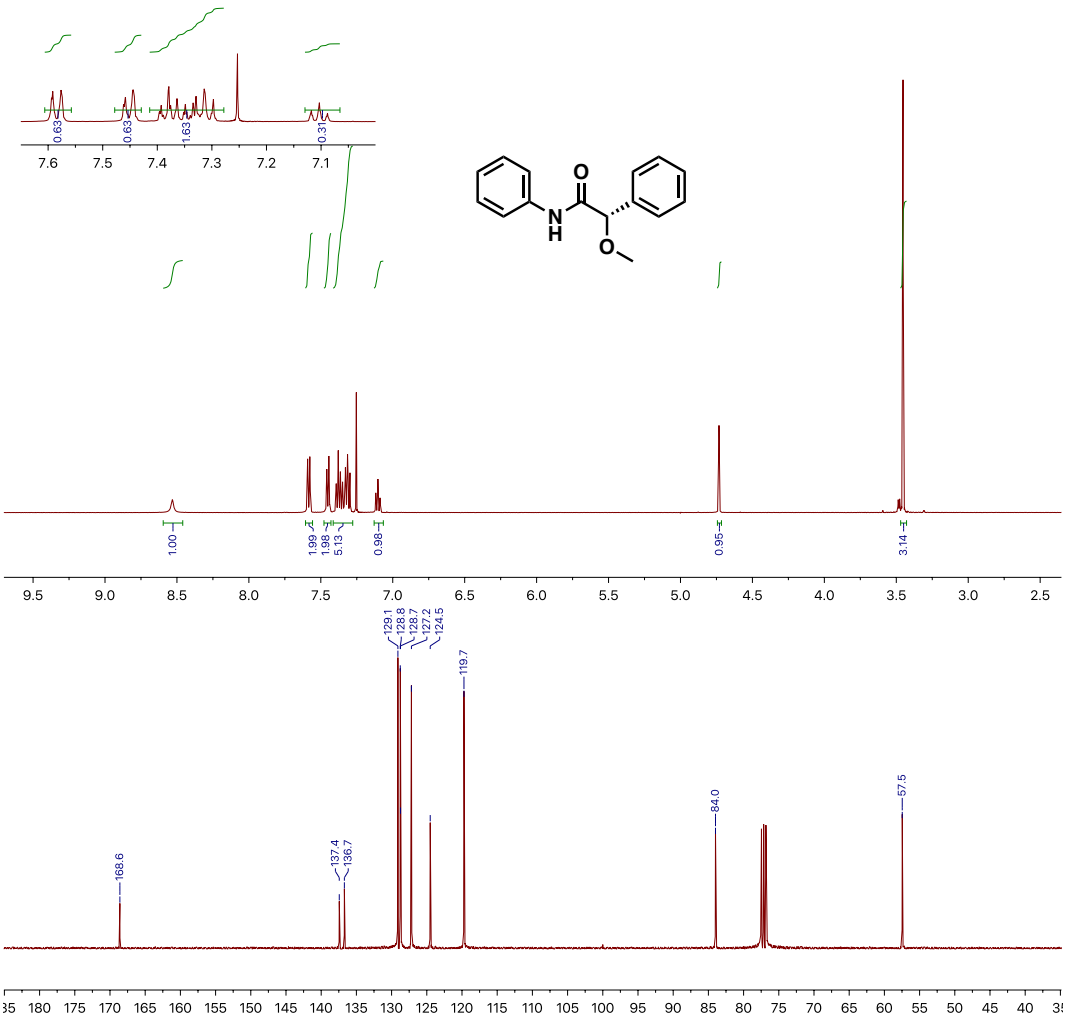

Figure S2. ^{1}H and ^{13}C NMR spectra of initiator **2*S*** in $CDCl_3$ (500 MHz and 125 MHz respectively).

3.3. Polymerization.

Poly-**1*R*** and poly-**1*S*** were synthesized by polymerization of 3-MeOPI with the lithium amide of **2*R*** (Li-**2*R***) or **2*S*** (Li-**2*S***) in a similar manner to that reported previously (Figure 1b).[S2] A typical polymerization procedure is described below and the polymerization results are summarized in Table S1.

3-MeOPI (386 μL, 3.0 mmol) and THF (4.8 mL) were placed in a glass ampoule with a three-way stopcock using a syringe and then the solution was cooled to –98 °C. Polymerization was initiated by adding Li-**2*R*** or Li-**2*S*** in THF (0.55 M), which was prepared by adding an equimolar amount of *n*-BuLi in hexane to solution of **2*R*** or **2*S*** in THF at 0 °C, via syringe. The reaction mixture was rapidly stirred for 50 min at –98 °C, and then polymerization was terminated by adding an excess amount of acetyl chloride (430 μL, 6.0 mmol). The reaction mixture was held at –98 °C for 15 min and then, 78 °C for 1 h to ensure complete termination. The mixture was poured into a large amount of MeOH-1 M HCl (50/1, v/v). The precipitated polymeric product was collected by centrifugation and dried *in vacuo* at rt. The degrees of polymerization (DP) of the obtained poly-**1*R*** and poly-**1*S*** were estimated to be 31 and 28, respectively, by ^{1}H NMR analysis using the peak intensity of aromatic region (7.20–5.40 ppm) involving [(4H, PIC)$_n$ + 5H (Ar Aniline)] ("n" is the number of PIC units in the polymer chain) relative to that of the aromatic proton resonances of the terminal MPA residue (3H, OMe MPA, 3.3 ppm) (Figure S3).

Poly-**3*S*** was also prepared according to the previously reported method (see run 3 in Table S1).[S2]

Table S1. Polymerization results of 3-MeOPI with Li-**2*R*** and Li-**2*S*** in THF at –98 °C[a]

run	Initiator	polymer				
		sample code	yield (%)[b]	n[c]	$M_n \times 10^{-3}$[d]	M_w/M_n[d]
1	Li-**2*R***	poly-**1*R***	59	31	3.8	1.3
2	Li-**2*S***	poly-**1*S***	52	28	3.1	1.2
3	Li-MMP	poly-**3*S***	47	33	4.3	1.2

[a][3-MeOPI] = 0.67 M, [3-MeOPI]/[Initiator] = 5 (runs 1 and 2), 10 (run 3). [b]Hexane–ethanol (3/1, v/v) insoluble part. [c]DP determined by ^{1}H NMR in $CDCl_3$. [d]Determined by SEC (polystyrene standards).

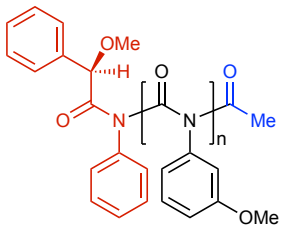

poly-**1*R***

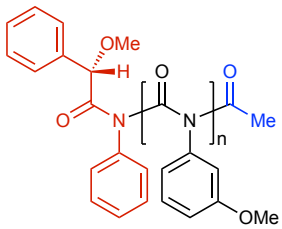

poly-**1*S***

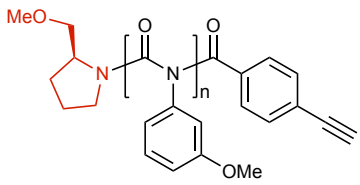

poly-**3*S***

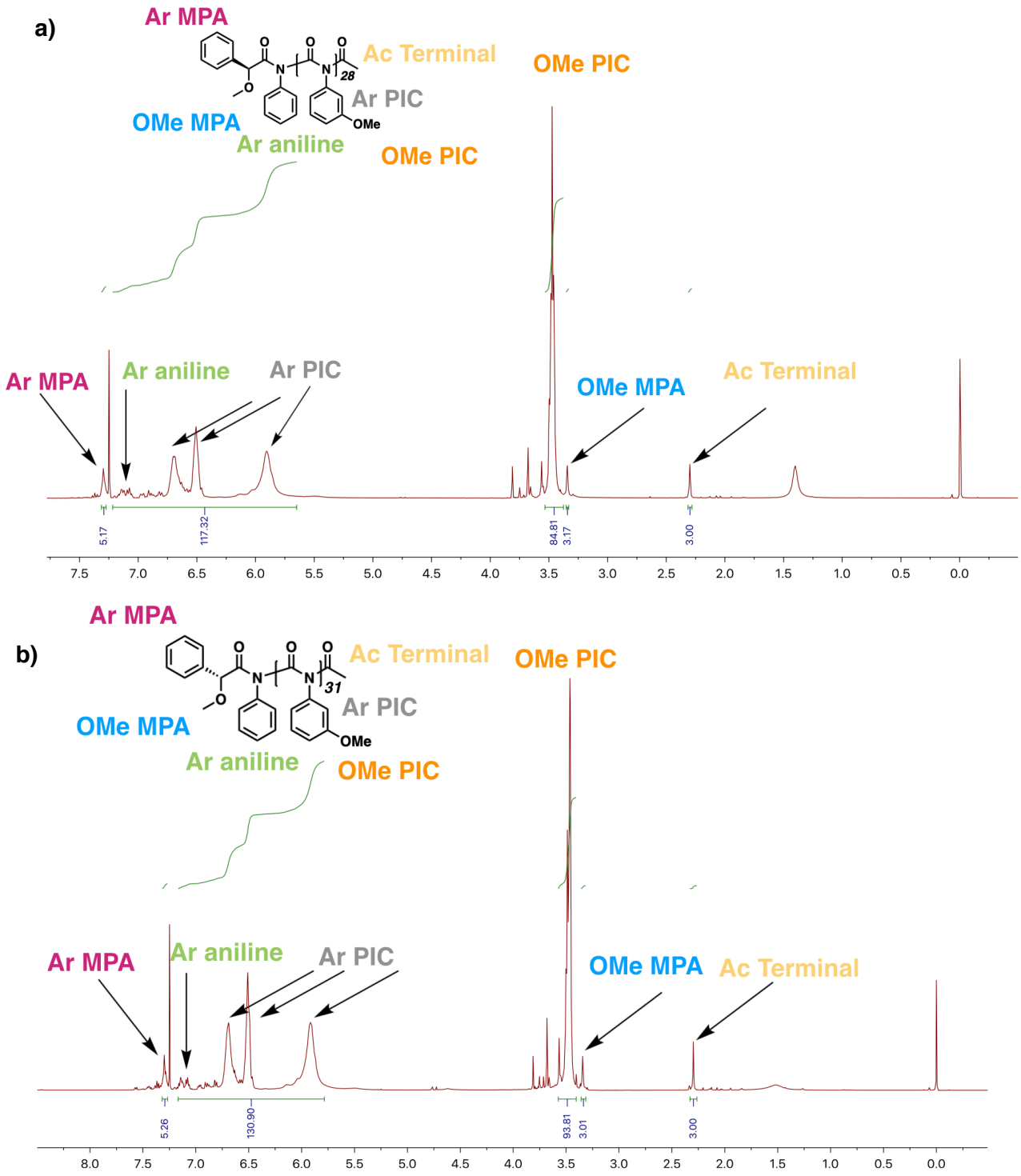

Figure S3. ^{1}H NMR (500 MHz) spectrum of (a) poly-**1*R*** (n = 31) and (b) poly-**1*S*** (n = 28) (500 MHz, $CDCl_3$).

4. Solvent Effect on the Conformational Composition of MPA Moiety

The employed solvents were classified according to their polarity and their donor/acceptor proprieties following Guttmann (AN/DN) values. As depicted in the graphs below the conformational switch is triggered by a delicate interplay of polar and donor effects. For detailed explanation on the classification of the solvents see references S3 and S4.

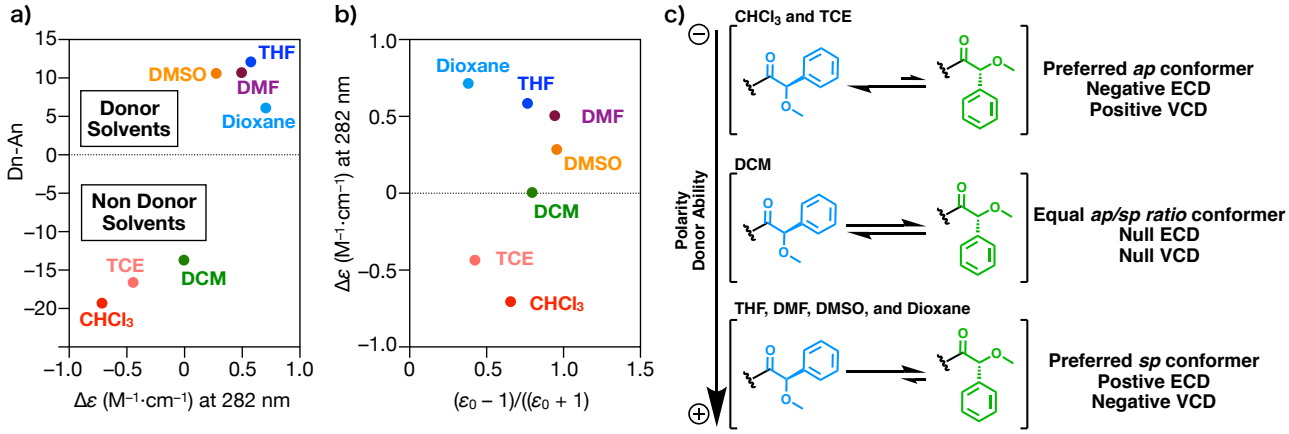

Figure S4. a) Classification of the solvents in donor/non-donor: plot of the Dn-An value against the $\Delta\varepsilon$ for poly-**1*R***. b) Classification of the solvents by polarity: plot of the $(\varepsilon\text{-}1)/(\varepsilon+1)$ (being ε the dielectric constant of the solvent) value against the $\Delta\varepsilon$ for poly-**1*R***. c) Schematic illustration of the conformational changes in the MPA moiety of poly-**1*R*** by the aforementioned donor/polar effects.

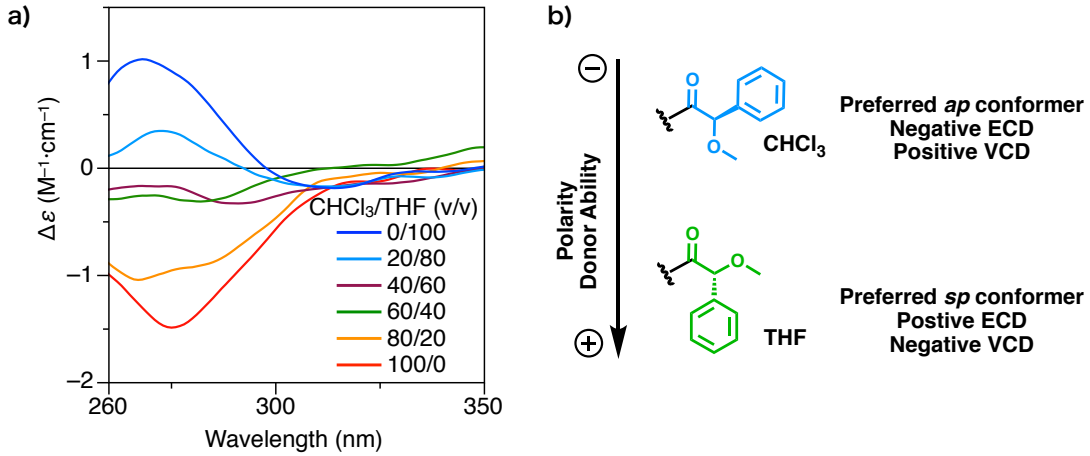

Figure S5. a) CD graph of the titration experiment between $CHCl_3$ and THF. b) Conceptual representation of the conformational change at the MPA moiety by tuning the $CHCl_3$/THF ratio.

5. IR Study on the Coordination of Li^+ to Poly-1*R*

Information of the MPA moiety could not be extracted from IR experiments due to the low ratio of MPA/isocyanate unit (*ca.* 1/28 for poly-**1*R***, see Table S1), precluding the observation of the C=O and OMe bands of the MPA unit due to overlapping with the main chain signals. However, IR experiments showed clear variations in the C=O stretching band of the polymer backbone (Figure S6). This shifting indicates that the coordination of Li^+ is happening not only in the MPA moiety at the α-end but also in the carbonyl groups along the polymer backbone.

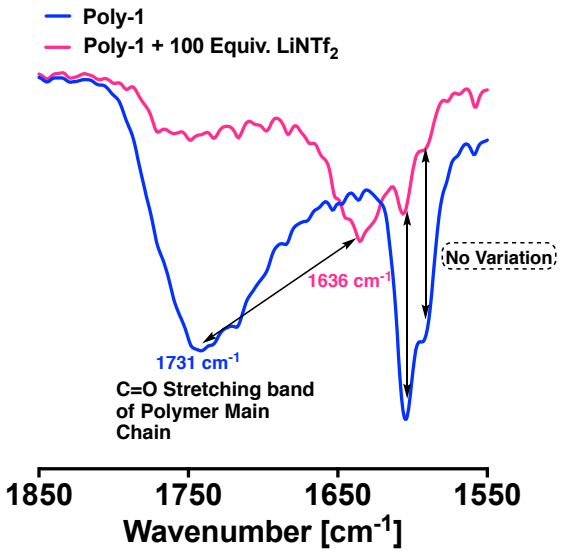

Figure S6. IR spectra of poly-**1*R*** before and after the addition of $LiNTf_2$, highlighting the variation in the stretching band of the PIC backbone.

6. IR and VCD Calculations

The detailed procedure for the construction of the initial 8_3 (eight units per three turn) poly(phenyl isocyanate) helical model was previously reported.[S5] The initial model of the left-handed (*M*) poly(phenyl isocyanate) (10 mer) was thus optimized by using molecular mechanic studies (MM) with an universal force field from the material studio program (Biovia) and further the density functional theory (DFT) method at the B3LYP/6-31G(d) level in Gaussian 09 program.[S6] The main chain torsion angles and stick model representation of the optimized structure are depicted in the main manuscript (Figure 4). In order to obtain accurate energies and IR/VCD spectra for the optimized structure, frequency analyses were performed using the computational methods explained above. The corresponding spectra were constructed from calculated dipole and rotational strengths assuming a Lorentzian band shape with a half-width at maximum of 4 cm^{-1}. The calculated frequencies were scaled by a frequency independent factor of 0.9613.[S7]

7. Supporting Data

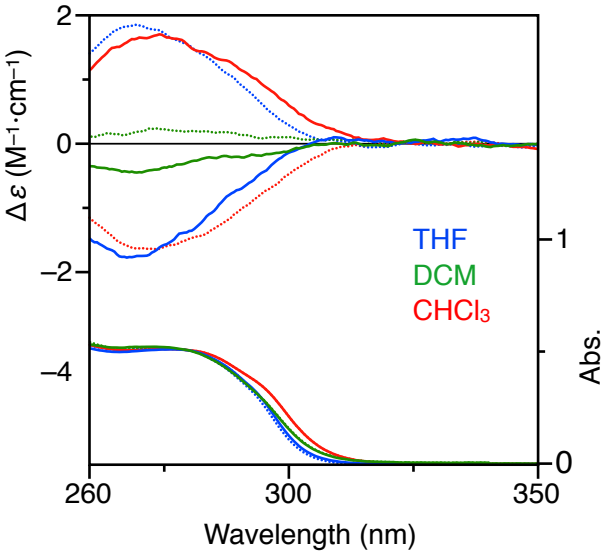

Figure S7. ECD and UV spectra of poly-**1*S*** (solid line) and poly-**1*R*** (dotted line) (0.2 mg/mL) in THF (blue), DCM (green), and $CHCl_3$ (red) at –10 °C.

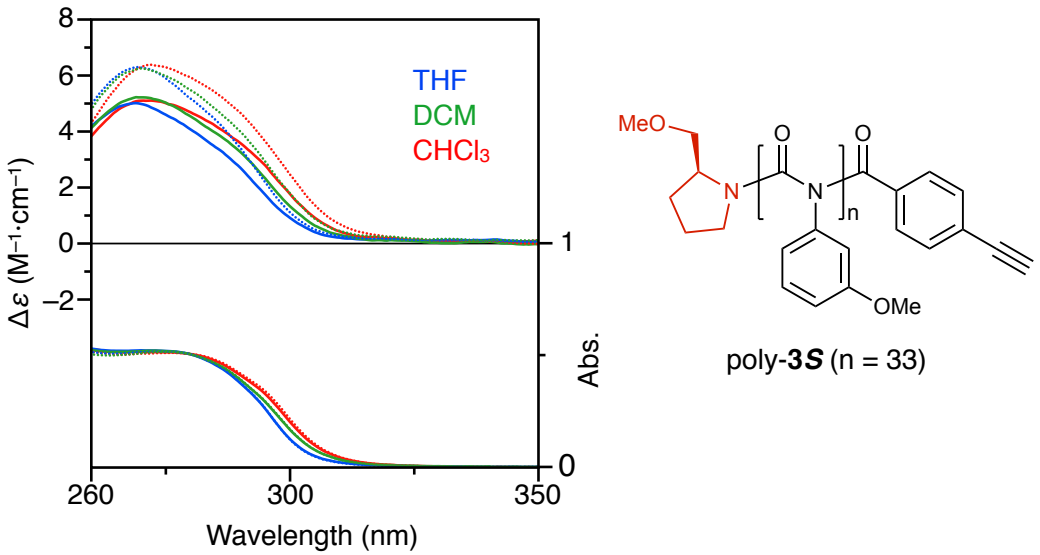

Figure S8. ECD and UV spectra of poly-**3*S*** (0.2 mg/mL) in THF (blue), DCM (green), and $CHCl_3$ (red) at 25 °C (solid line) and –10 °C (dotted line).

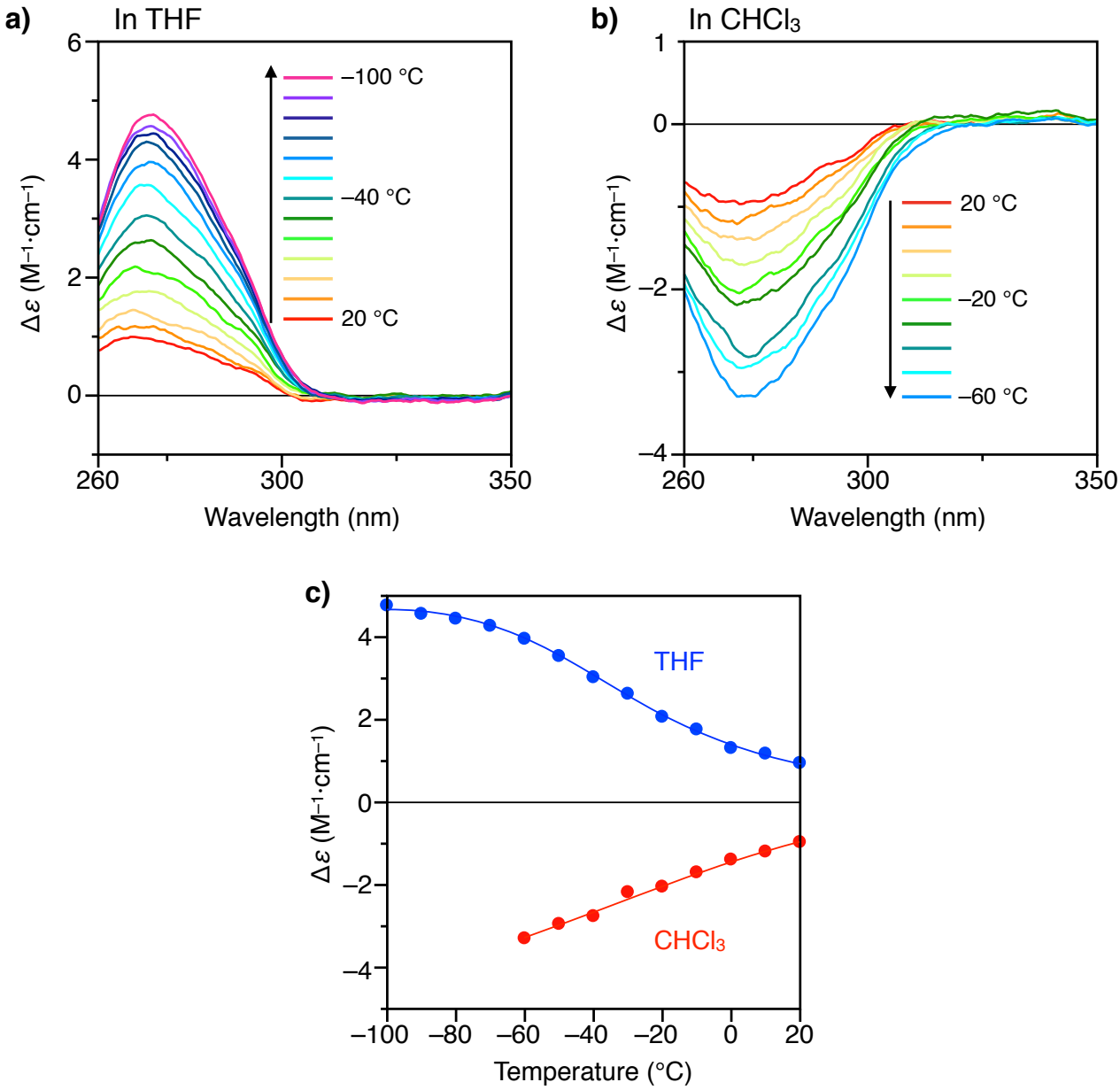

Figure S9. a, b) VT-ECD spectra of poly-**1*R*** (0.2 mg/mL) in $CHCl_3$ (a) and THF (b). c) Plots of the CD intensity ($\Delta\varepsilon_{max}$) of poly-**1*R*** in $CHCl_3$ and THF versus temperature.

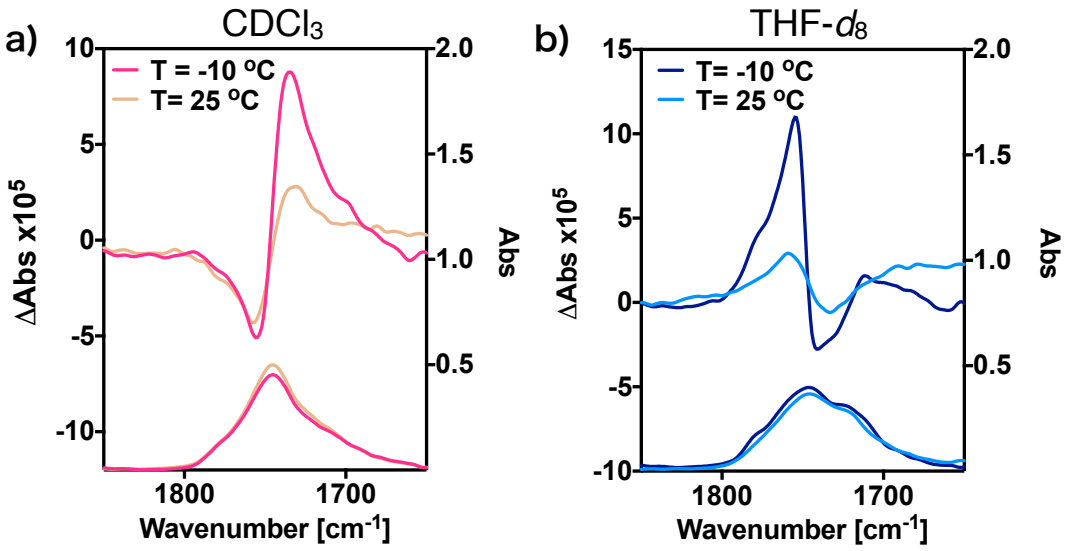

Figure S10. VCD studies for poly-**1*R*** (25 mg/mL) in $CDCl_3$ and THF-d_8 (a and b respectively) at –10 and 25 °C. These results are in full agreement with the helical sense enhancement process mediated by thermal decreasing inferred by VT-ECD experiments shown in the main manuscript.

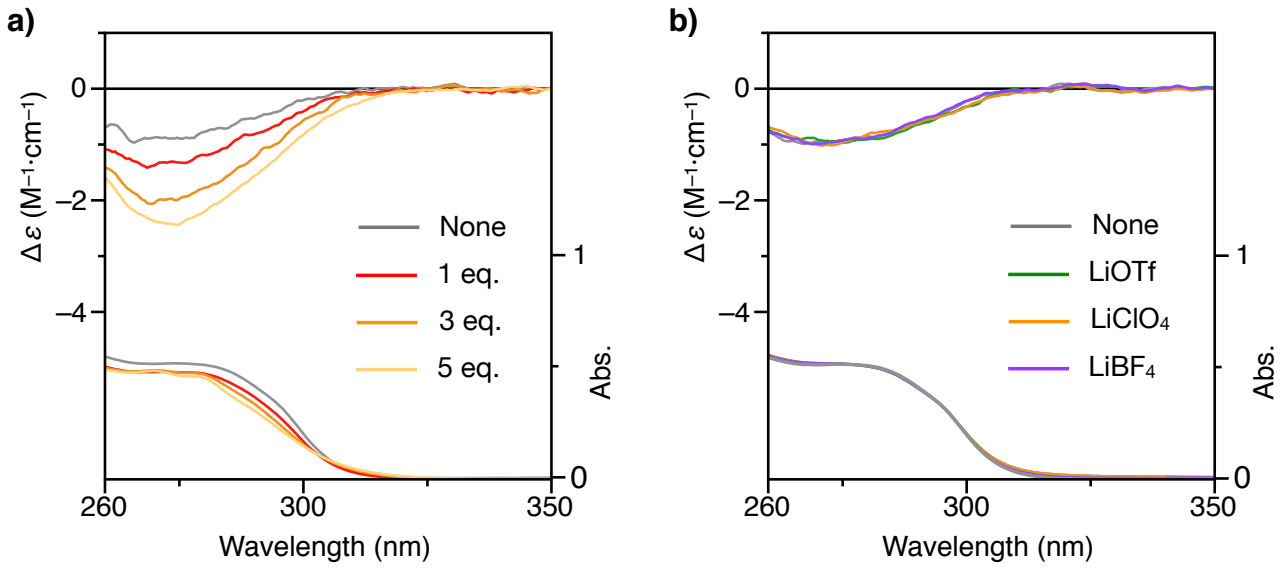

Figure S11. (a) ECD and UV titration of poly-**1*R*** (0.2 mg/mL) in $CHCl_3$ with LiBArF in THF ($CHCl_3$/THF = 500/1,v/v) at 25 °C. (b) ECD and UV spectra of poly-**1*R*** (0.2 mg/mL) in $CHCl_3$ in the absence and presence of LiOTf, $LiClO_4$, $LiBF_4$ ([Li salt]/[poly-**1*R***] = 20) at 25 °C. The $\Delta\varepsilon$ and ε values were calculated using the concentration based on the monomer unit.

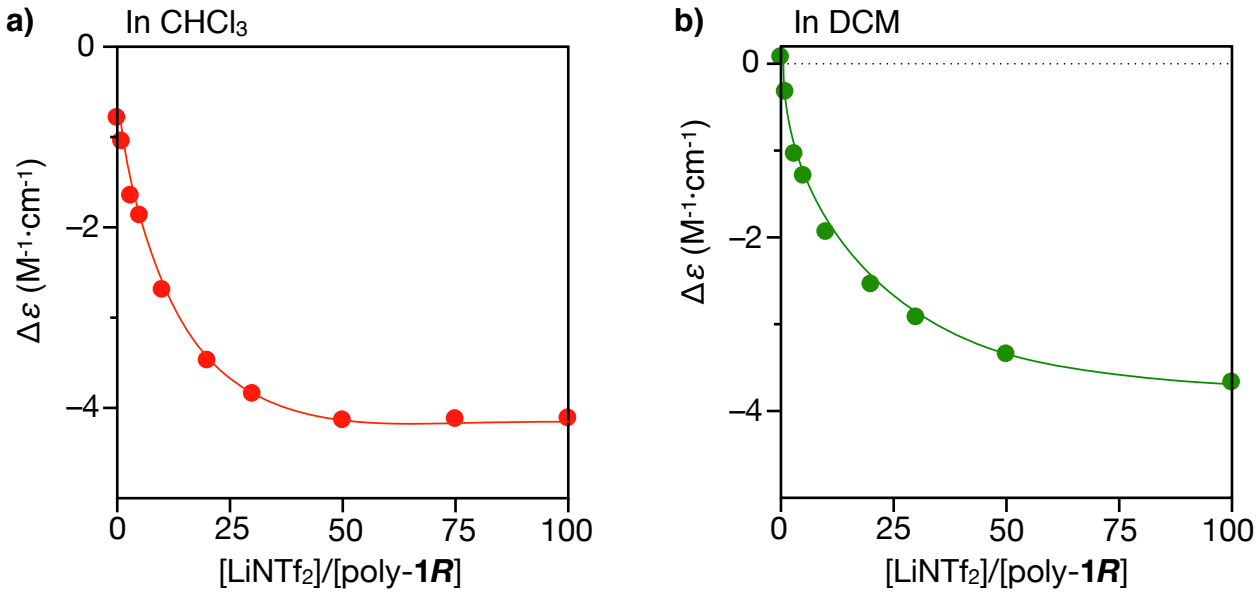

Figure S12. Plots of the CD intensity (Δε at 272 nm) of poly-**1*R*** (0.2 mg/mL) with $LiNTf_2$ in $CHCl_3$ (a) and DCM (b) at 25 °C. The Δε and ε values were calculated using the concentration based on the monomer unit.

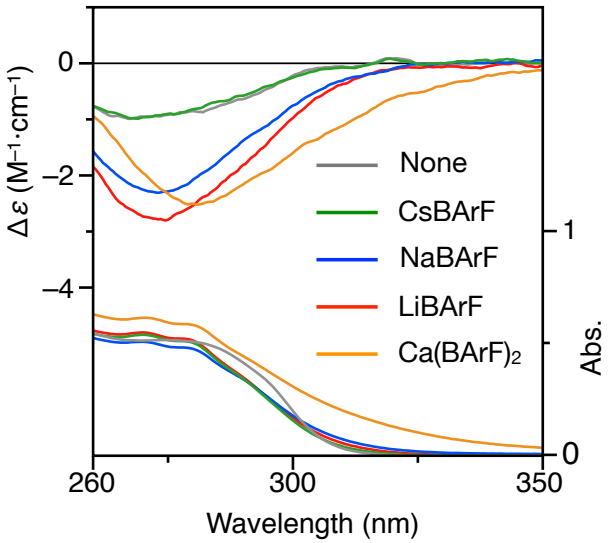

Figure S13. ECD and UV spectra of poly-**1*R*** in $CHCl_3$ (0.2 mg/mL) with 5.0 eq. of various BArF salts in THF ($CHCl_3$/THF = 500/1,v/v) at 25 °C. The Δε and ε values were calculated using the concentration based on the monomer unit.

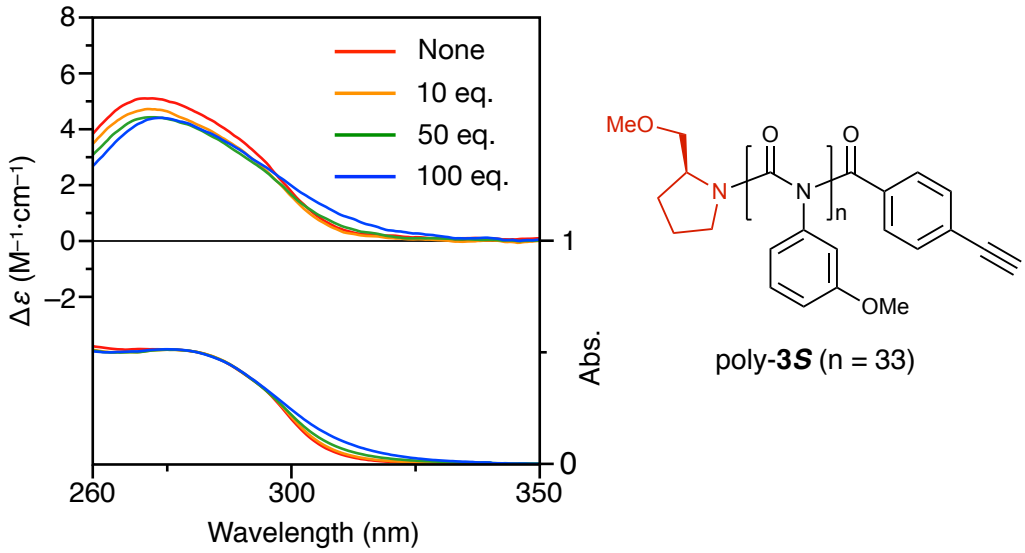

Figure S14. ECD and UV titration of poly-**3*S*** (0.2 mg/mL) in $CHCl_3$ with $LiNTf_2$ at 25 °C.

8. Supporting References

S1. a) O. Shyshov, R. C. Brachvogel, T. Bachmann, R. Srikantharajah, D. Segets, F. Hampel, R. Puchta and M. von Delius, *Angew. Chem., Int. Ed.* 2017, **56**, 776-781. b) D. Hirose, A. Isobe, E. Quiñoá, F. Freire and K. Maeda, *J. Am. Chem. Soc.*, in press.

S2. a) K. Maeda, S. Wakasone, K. Shimomura, T. Ikai and S. Kanoh, *Chem. Commun.* 2012, **48**, 3342-3344. b) K. Maeda, S. Wakasone, K. Shimomura, T. Ikai and S. Kanoh, *Macromolecules* 2014, **47**, 6540-6546.

S3. S. Leiras, F. Freire, J. M. Seco, E. Quinoa and R. Riguera, *Chem. Sci.* 2013, **4**, 2735-2743.

S4. a) O. W. Kolling, *Anal. Chem.* 1978, **50**, 212; b) C. Reichardt, Solvent and Solvent Effects in Organic Chemistry, Wiley-VCH, Weinheim, 2003.

S5. J. A. Young and R. C. Cook, *Macromolecules* 2001, **34**, 3646-3653.

S6. Gaussian 09, Revision E.01, M. J. Frisch, G. W. Trucks, H. B. Schlegel, G. E. Scuseria, M. A. Robb, J. R. Cheeseman, G. Scalmani, V. Barone, B. Mennucci, G. A. Petersson, H. Nakatsuji, M. Caricato, X. Li, H. P. Hratchian, A. F. Izmaylov, J. Bloino, G. Zheng, J. L. Sonnenberg, M. Hada, M. Ehara, K. Toyota, R. Fukuda, J. Hasegawa, M. Ishida, T. Nakajima, Y. Honda, O. Kitao, H. Nakai, T. Vreven, J. A. Montgomery, Jr., J. E. Peralta, F. Ogliaro, M. Bearpark, J. J. Heyd, E. Brothers, K. N. Kudin, V. N. Staroverov, R. Kobayashi, J. Normand, K. Raghavachari, A. Rendell, J. C. Burant, S. S. Iyengar, J. Tomasi, M. Cossi, N. Rega, J. M. Millam, M. Klene, J. E. Knox, J. B. Cross, V. Bakken, C. Adamo, J. Jaramillo, R. Gomperts, R. E. Stratmann, O. Yazyev, A. J. Austin, R. Cammi, C. Pomelli, J. W. Ochterski, R. L. Martin, K. Morokuma, V. G. Zakrzewski, G. A. Voth, P. Salvador, J. J. Dannenberg, S. Dapprich, A. D. Daniels, Ö. Farkas, J. B. Foresman, J. V. Ortiz, J. Cioslowski, and D. J. Fox, Gaussian, Inc., Wallingford CT, 2009.

S7. F. Anthony, P. Scott, L. Radom, *J. Phys. Chem.* 1996, **100**, 16502-16513.